ICAS 2020 SHANG HAI
International Council of the Aeronautical Sciences
32nd Congress of the International Council of the Aeronautical Sciences
September 6-10, 2021
Pudong Shangri-La, Shanghai, China

STUDY OF COMPOSITE SKIN-STRINGER FATIGUE BEHAVIOR UNDER BROADBAND RANDOM VIBRATION

Stanislav Dubinskii[1], **Filipp Sevastyanov[1]**, Vladimir Kostenko[1], Stanislav Denisov[1], Ivan Zharenov[1]

[1]*The Central Aerohydrodynamic Institute named after N.E. Zhukovsky (TsAGI), 1, Zhukovsky str. Zhukovsky, Moscow Region, 140180, Russian Federation*

Abstract

The study is focused on experimental and analytical evaluation of dynamic response of composite structure, subjected to broadband random vibration. The number of studies on this particular topic is relatively small, though the understanding of structure response to jet noise and generating of related S-N data are essential for composite aircraft sonic fatigue certification.

Keywords: composite structure, vibroacoustic loading, finite element model, fatigue, S-N curve.

1. Intoduction

The problem of studying the fatigue characteristics of aircraft structures under vibroacoustic loads originates in the late 1950s - early 1960s. Then, as a result of the active introduction of gas turbine engines in aviation, along with an increase in the power of power plants, there was also a significant increase in the loads associated with vibrations and acoustic noise, which led to the occurrence of fatigue fractures [1].

The phenomenon of vibroacoustic fatigue implies a relatively low level of stresses arising in the structure at very high loading frequencies. In this case, the loading spectra are most often random in a wide frequency range. Based on this, the problem of studying the fatigue characteristics of aircraft structures under vibroacoustic loads requires the use of special approaches to its solution. So, in the 1960-1970s, a large number of theoretical and experimental studies were carried out to study the properties of various materials and structures created on their basis, subjected to acoustic or vibration loading of various nature. The result of these studies was the development of industry reference books and manuals [2-3], which are now actively used in the aviation industry.

Most of the research in those years was devoted to traditional metal materials and structures. However, the tendency of the late 20th - early 21st century to actively introduce and increase the variety of used composite materials in aircraft construction requires additional research.

The main advantage of composite structures is the high ratio of their elastic-strength characteristics to mass characteristics. At the same time, the fatigue characteristics of composite structures largely depend on their internal structure, including at the microlevel. Impact damage is the critical factor in terms of effect on fatigue and damage tolerance of a composite structure [4-6]. That is why, when certifying civil aviation equipment, both in accordance with local and foreign requirements, it is necessary to carry out a large amount of work related to the study of the effect of impact damage on the strength and damage tolerance of the structure.

The accumulated experience in researching the fatigue characteristics of aircraft structures under vibroacoustic loads has shown that a "skin-stringer" sample or "T-sample" can be selected as the lower-level samples in the "Building Block" methodology [7-10]. Such a sample makes it possible to simulate the bending vibration mode prevailing in the structure, which is realized in the classical cellular airframe assembly of the empennage, wing, and fuselage under vibroacoustic loading.

The purpose of this work is to study the fatigue characteristics of a composite structure, including the effect of impact damage, for a typical structural stress concentrator ("T-sample").

2. Finite element model

The finite element modeling was carried out using Abaqus software. The model of the T-sample consisted of 8-nodal hexagonal solid elements. The choice of this type of finite elements is due to the need for a more accurate calculation of shear and bending deformations. The model consisted of 4352 elements (8258 nodes).

The stacking was modeled by discretizing into one finite element across the thickness of composite layup for both skin and stringer (9 plies in one element total). For each ply, its individual parameters were defined separately (fiber orientation, thickness, number of integration points). It was assumed that the sample has a constant thickness, all bonds between the plies are absolutely rigid, and the interlaminar strength was not taken into account. The tension and compression elastic modulus of the plies was assumed to be the same.

To determine the eigenmodes and eigenfrequencies of oscillations of the finite element model, modal analysis was performed at the first stage, for which the Lanczos direct block method [11-12] and the subspace iteration method [11-12] were used, which showed identical results. Modal analysis was done in the selected frequency range (50…1550 Hz), based on the restrictions on the operating modes of the shaker (electrodynamic shaker Derritron VP30), used for vibration testing. The damping coefficient used in FEM was calculated from the equation:

$$\beta_n = \frac{1}{\sqrt{1+\left(2\pi/\delta\right)^2}} \tag{1}$$

where δ is the logarithmic damping decrement, which was determined experimentally by measuring the amplitude of free damped oscillations from a half-sine pulse with a duration of ~2–5 ms by the formula

$$\delta = \frac{1}{n}\ln\frac{A_0}{A_n} \tag{2}$$

where A_0 is the oscillation amplitude at an arbitrary time t and A_n is the amplitude after n oscillation cycles at time (t + n * T), where T is the oscillation period.

The resulting oscillation eigenmodes and eigenfrequencies were used to calculate the dynamic response of the T-sample by determining the field of root-mean square (RMS) values of relative strains. The vibration effect at each node of the finite element model was set by the spectral density function of accelerations. Moreover, it was assumed that the loading is steady, ergodic, and completely correlated over the sample surface. As a result of the calculation, the accelerations and displacements of the model nodes were determined, which, with a known stiffness matrix for each element, made it possible to calculate stresses and relative strains in each ply.

3. Test Specimen

For testing the single-stringer panels (T-sample) were taken (Figure 1), the skin and stringer of which consist of eight plies of HexPly carbon fiber (M21/34%/UD194/IMA superscript “c”) and one ply fiberglass (M21/45%/120 superscript “g”) prepreg. Both the skin and stringer has the stacking sequence ($0°^g$, $\pm45°^c$, $0°^c$, $90°^c$, $0°^c$, $0°^c$, $\pm45°^c$). The noodle in the root of the joint is made of carbon fiber M21/34%/UD194/IMA. The mechanical properties of the ply for these materials are given in Table 1.

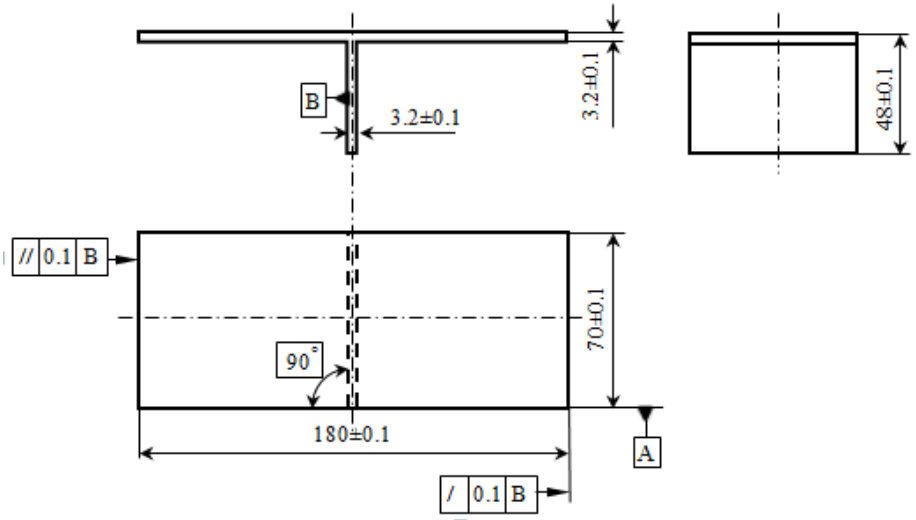

Figure 1 – Sketch of T-sample (all the length units are in mm)

Table 1 – Mechanical properties of the ply

	E_{11}, GPa	E_{22} / E_{33}, GPa	υ_{12} / υ_{13} / υ_{23}	G_{12}, GPa	G_{13} / G_{23}, GPa	Density, kg/m^3
M21/34%/UD194/IMA	162.0	9.3	0.33	5.4	3.5	1580
M21/45%/120	28.6	8.7	0.33	3.1	3.1	1770

4. Experimental

To experimentally study the behavior of the composite T-sample under vibration loading conditions, a special stand was assembled with a computer control system that set the excitation of the required form and measured the response parameters. The sample was rigidly fixed on the shaker table with a clamp. Two accelerometers and four strain gauges were installed on the sample, and another accelerometer was located directly on the shaker table.

The procedures for generating signals and processing data were implemented via the functions of the Advanced Analysis Library of the LabWindows/CVI commercial software package (National Instruments) [13]. The signal was formed by a digital-to-analog converter as a sequence of blocks with discrete values. The dataset for each block was obtained by software generation of a sampling of pseudorandom numbers with a normal distribution law and subsequent digital filtering. The result was a random signal with a uniform spectral density in the given frequency band.

5. Results of modal and dynamic analysis

The calculation showed that the first six modes were located in the considered frequency range 50…1550 Hz (Figure 2). Taking into account the fixation and loading conditions of the specimen on the test bench, resonant oscillations can arise only in a mode symmetric about the stringer axis. Figure 3b shows the only form symmetric about the stringer axis in the selected frequency range – the bending form at the 2nd eigenfrequency of 300 Hz.

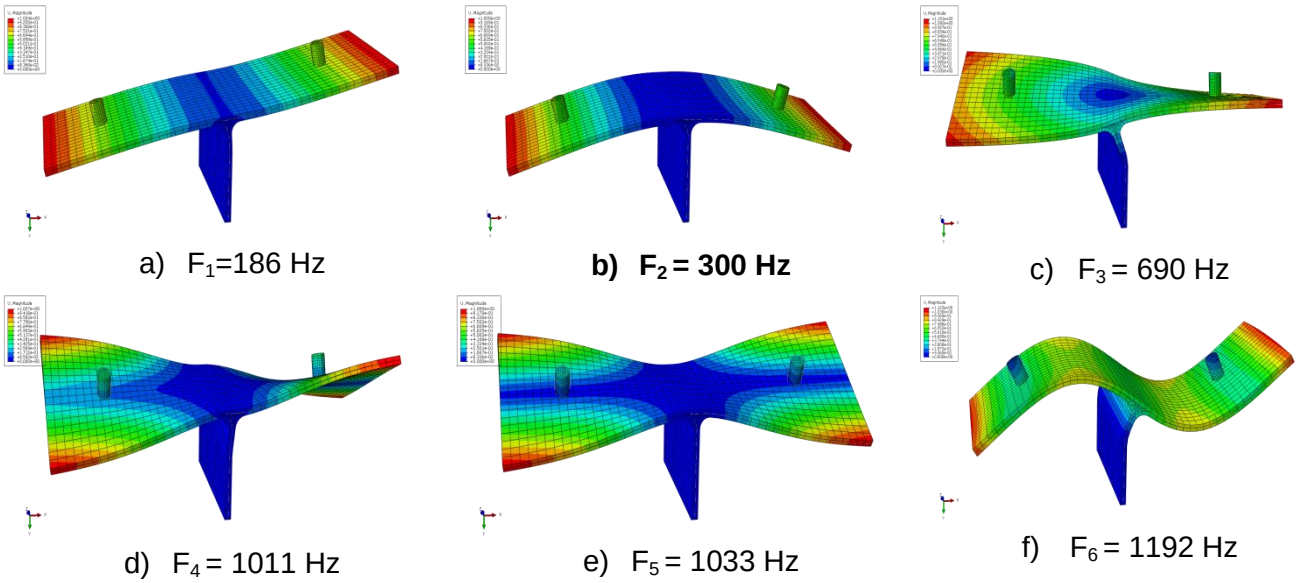

a) F_1=186 Hz **b) F_2 = 300 Hz** c) F_3 = 690 Hz

d) F_4 = 1011 Hz e) F_5 = 1033 Hz f) F_6 = 1192 Hz

Figure 2 – All the six eigenmodes of T-sample in considered frequency range obtained by analysis

In order to validate the shape of the first symmetrical resonance mode obtained by calculation, using a portable stroboscope Testo 477, video was taken with the sample executing sinusoidal oscillations with a frequency 300 Hz and a driving force amplitude of 5 g (where g = 9.80665 m/s^2 is gravitational acceleration). Analysis of the video showed that the shape of oscillation of the sample on the experimental stand corresponds to the mode of the 2nd eigenfrequency obtained by finite element calculations (Figure 3).

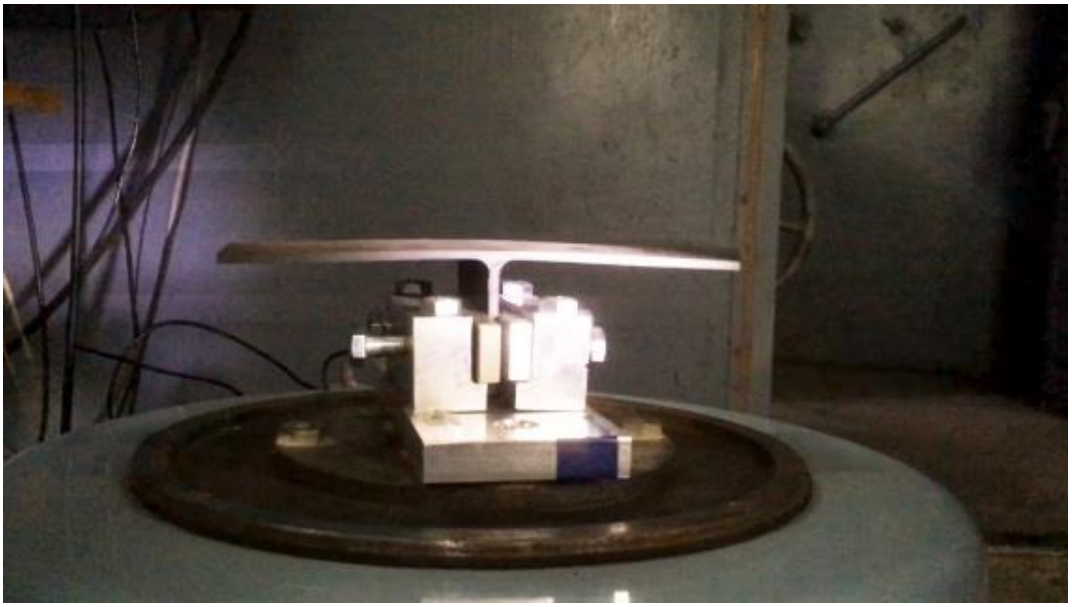

Figure 3 – Oscillation shape of T-sample on the shaker

Using finite element modeling, the stress-strain state of the T-sample was evaluated for the prevailing oscillation mode. It was found that plies No. 5 and No. 14, laid at 90° to the stringer axis, are the most loaded - they have maximum stresses during oscillations at the resonant frequency. Since the installation of strain gauges is possible only on the surface of the sample, the surface deformations were also evaluated in order to select the location of the strain gauges on the T-sample. The largest strains in the sample occur on its lower surface — in the stringer–skin joint zone (Figure 4a); however, it is technically difficult to install strain gauges in this area, so a symmetrical zone of maximum strain on the upper surface was chosen (Figure 4b). The finite element calculation took into account the influence of the geometry and mass of the sensors on the stiffness and inertial characteristics of the sample. The strain gauges were simulated as a thin rectangular plate of a single finite element adhesively bonded to the T-sample and receiving the strains from the sample. The accelerometers were simulated as a volumetric cylindrical body with a given density (ρ = 6650 kg/m^3) and stiffness (E = 1070 GPa, v = 0.3) (Figure 5).

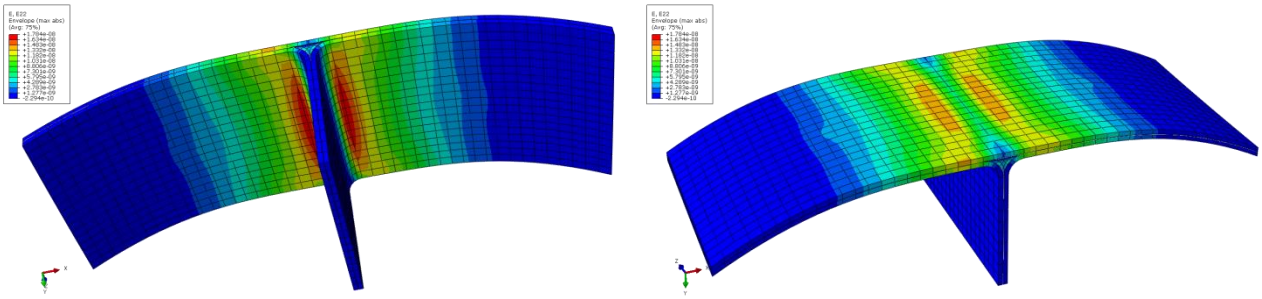

a) *b)*

Figure 4 – Estimation of strains at first symmetrical resonance frequency: (a) strains on lower surface, (b) strains on upper surface

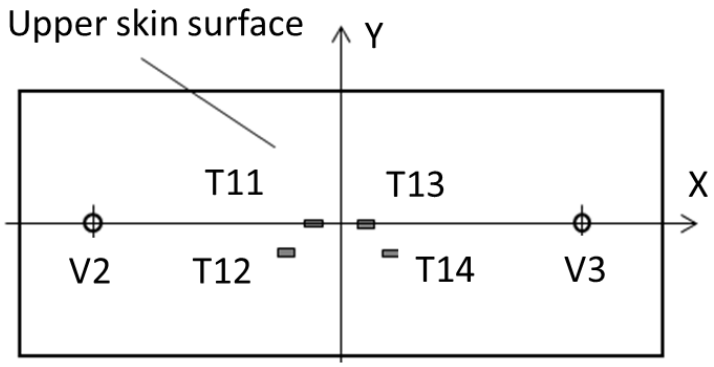

Sensor number	X, mm	Y, mm
V2	-60	0
V3	60	0
T11	-5	0
T12	-10	-10
T13	5	0
T14	10	-10

Figure 5 – Installation zone of accelerometers (V2, V3) and strain gauges (T11-T14).

The empirical value of the first symmetrical resonance frequency was determined for oscillations excited by a sinusoidal signal of constant level with gradually increasing frequency in the given range. The excitation and response signals from the accelerometers mounted on the shaker and the sample were continuously monitored. The value of the resonance frequency was taken as the frequency of maximum acceleration in the spectrum of the signal from the sensor installed at the reference point, calculated by Fourier transform. Table 2 compares the values of the first symmetrical resonance frequency obtained by calculation and experiment.

Table 2 – Values of first resonance frequency

Parameter	Experiment	Calculation
Second eigenfrequency / first resonance frequency f_R, Hz	296	300

The dynamic response of the sample was studied under conditions of random broadband loading in the frequency range of 50–1550 Hz at RMS acceleration levels of 4, 6, 8, and 12 g (where g = 9.80665 m/s^2). During the tests, data were continuously collected from measuring sensors with 16-bit digitization, a sampling frequency of 10000 points per second and a frequency resolution of 1.2207 Hz. The interval of the processed data, including the Fourier transform, was at least 20-30 seconds. Based on the data obtained, the values of the resonance frequency and PSD of the received signals were recorded. Figure 6a shows the power spectral density (PSD) of the given acceleration. Figure 6b shows the PSD of the acceleration obtained on accelerometer V2.

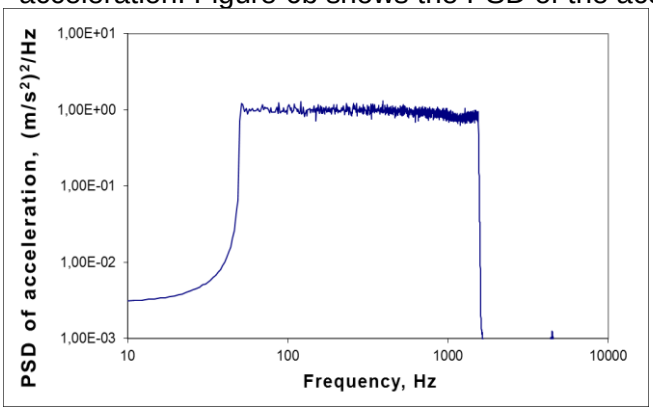

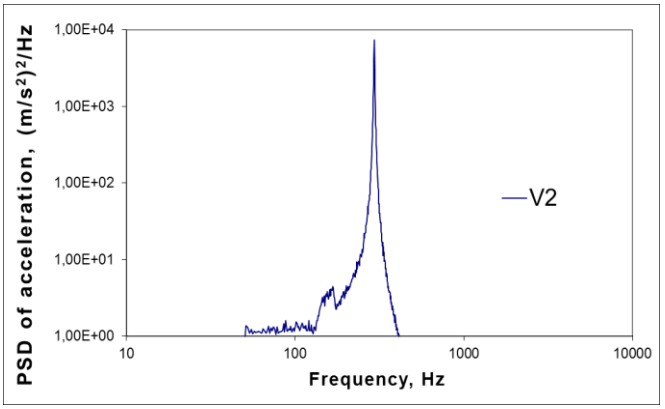

Figure 6 – Spectral density of broadband vibration loading: (a) reference signal at level of 12 g, (b) signal measured on accelerometer V2.

Comparison of the calculated RMS values of accelerations and strains on the surface of the T-sample with the experimentally measured values showed their good convergence: the error for strains does not exceed 5% and for accelerations – 15%.

6. Fatigue testing of T-samples

6.1 Failure criterion

An experimental study of the fatigue characteristics of T-samples was carried out on the shaker. The sample was loaded by the random narrow-band vibration with a bandwidth of 30 Hz and the average frequency at the first symmetric resonant frequency. Each sample was tested at a given level of RMS strains, which were monitored in real time by means of the strain gauges.

The failure criterion was a decrease in the resonance frequency by 2-3%, which is consistent with both foreign approaches [8] and local practice [14]. The accumulated experience has shown that such a frequency reduction in composite sample makes it possible to determine changes in the stiffness of the elastic system due to the initiation of internal microcracks. For such a decrease in the resonance frequency, the relative damage of the cross-section of the sample is 10–20%. With a further decrease in frequency by 10–15% the sample fracture is usually occurred [14].

When the resonance frequency dropped by 2%, the samples were subjected to a standard ultrasonic test (UT) procedure: uniaxial acoustic scanning (A-scan). After this, tests continued with periodic nondestructive testing until the appearance of visible defects.

6.2 Fatigue test results and S-N curve

Table 3 summarizes the fatigue test results of 10 samples; from the data therein, it follows that for the skin-stringer joint there is a clear relationship between the number of cycles to failure (fatigue failure) and the basic vibration load level. Based on the data in Table 3, using various probabilistic criteria, S-N curves for T-samples were plotted (Figure 7), and a comparison with data from ESDU 84027 [3] for samples of a similar configuration (integral stringer) was made.

Table 3 – Summary of fatigue test results

Sample number	RMS strain, μm/m	Cycles to failure
1	6000 (static)	1
2	1900	3,26E+03
3	1500	1,90E+05
4	1200	1,60E+06
5	1000	6,00E+06
6	950	7,20E+06
7	900	1,66E+07
8	850	2,38E+06
9	800	7,90E+06
10	600	1,04E+08

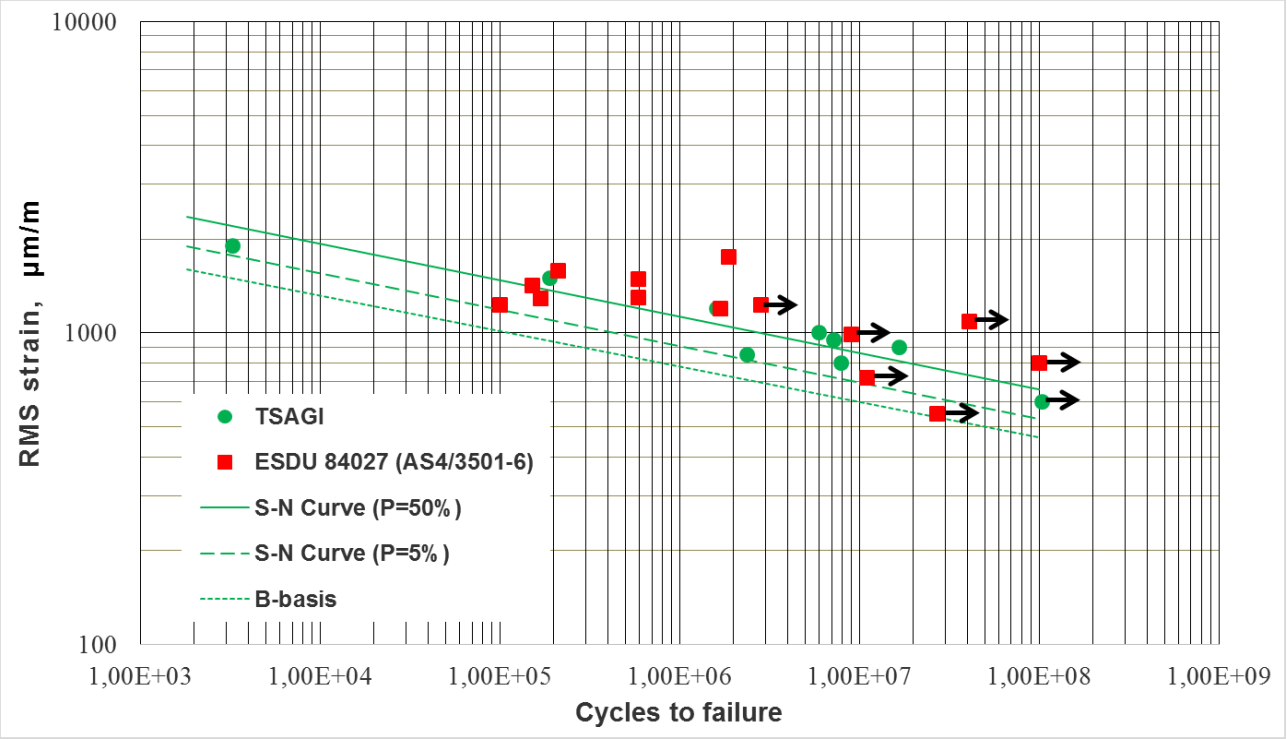

Figure 7 – The fatigue tests results vs. the ESDU data

6.3 Effect of the impact damage on fatigue of T-sample

To study the effect of the impact damage on fatigue characteristics of T-sample a batch of 10 samples was manufactured. Impact damage with energies of 5, 10, 20, and 30 J was applied using Instron CEAST 9350 with a 25 mm diameter identor. There were 2 points of impact: 1st - the geometric center of the upper surface of the skin and 2nd - zone of maximum strain in Figure 4b.

The fatigue testing of impacted samples was carried out on the same experimental stand with same loading conditions. Table 4 summarizes the fatigue test results for 10 impacted samples.

Table 4 – Summary of fatigue test results for impacted samples

Sample number	Energy of impact damage, J	RMS strain, μm/m	Cycles to failure
11	30 (center)	800	1,15E+04
12	20 (center)	600	7,49E+05
13	10 (center)	600	2,56E+06
14	10 (center)	800	2,93E+05
15	5 (center)	600	4,19E+07
16	5 (max strain zone)	600	1,36E+06
17	5 (max strain zone)	800	1,33E+05
18	5 (max strain zone)	500	1,39E+06
19	5 (max strain zone)	400	4,24E+07
20	5 (max strain zone)	700	2,03E+05

The comparison of the results for impacted and virgin samples is shown in Figure 8. From the data therein, it follows that the impact damage of 5 J significantly reduces the durability of composite “skin-stringer” joint under random vibration loading.

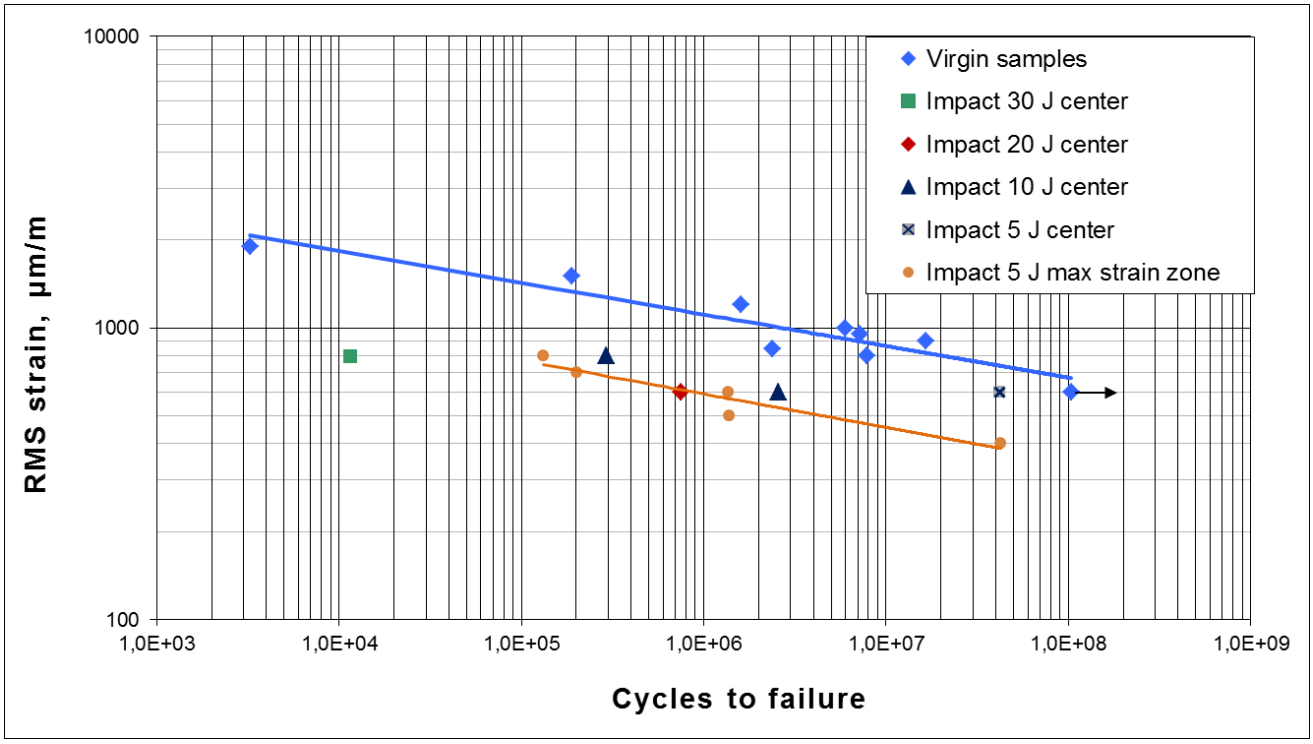

Figure 8 – The fatigue tests results of impacted T-samples

S-N curves for virgin and impacted (5 J) T-samples, respectively, can be interpolated using the following formulas:

$$RMS\ \varepsilon = 4996{,}2\ N^{-0{,}109}\ , \quad (3)$$

$$RMS\ \varepsilon = 2900{,}1\ N^{-0{,}115}\ , \quad (4)$$

where *RMS ε* is root mean square value of surface strain and *N* is the number of cycles to failure.

6.4 Damage growth and failure mode

The damage growth process was studied by the real-time monitoring of the eigenfrequency reduction during the fatigue testing, as it shown in Figure 9. There are 3 main points to consider: 1st is when failure criterion (2% eigenfrequency reduction) is triggered, 2nd is when delamination becomes visible on one side of T-sample and 3rd is when fatigue delamination became visible on both sides.

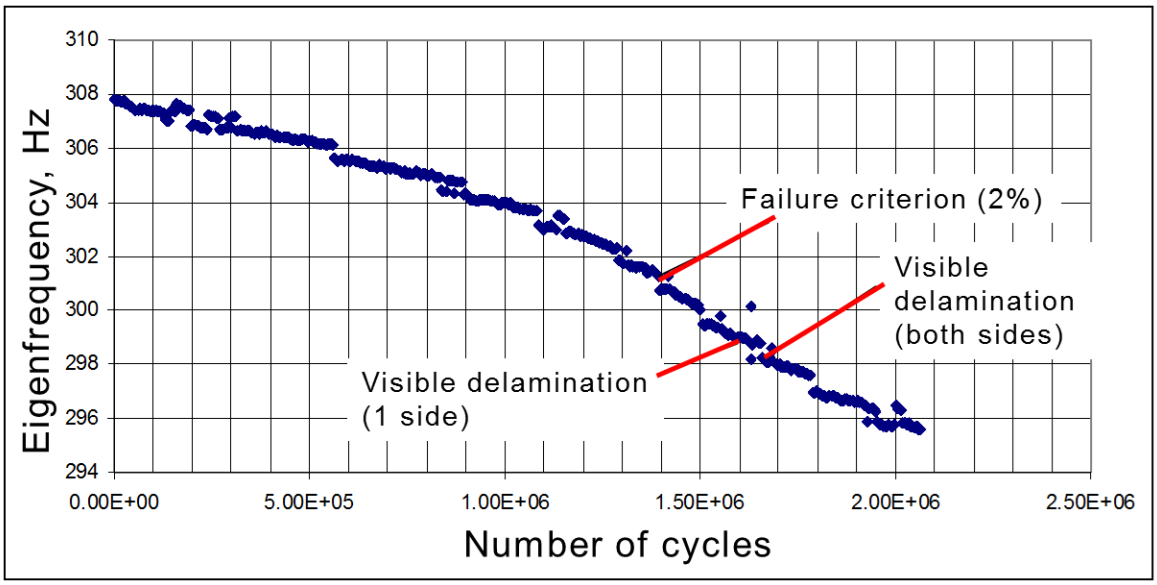

Figure 9 – Eigenfrequency reduction during the fatigue testing

Several different non-destructive testing methods were used to study the mechanisms of internal damage growth during fatigue testing of T-samples. One of these methods is vibrothermography

[15], which is based on measuring of the thermal field of a sample caused by vibration. The SC7700M thermal imager was used to record the thermal field of a T-shaped specimen during fatigue tests.

As the experiment showed, the applied method makes it possible to detect internal delamination in the sample due to the different heating rates of the damaged and undamaged parts of the sample, as shown in Figure 10. Such a defect is not detected visually or using the ultrasonic method, but it reduces the natural frequency of the sample by 2% (Figure 10b), so that, according to the chosen failure criterion, the sample is already considered “failed”. This is due to the fact that the failure of the sample begins in the radius zone of the joint, where the capabilities of the A-scan, designed to study the regular zones of the structure, are insufficient.

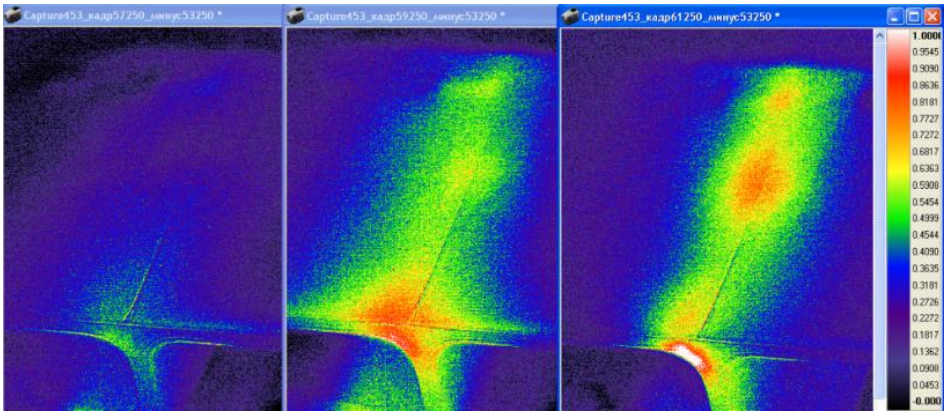

a) b) c)

Figure 10 – Damage growth registered by vibrothermography: (a) initial conditions (before fatigue testing), (b) internal delamination growth at N = 1,39E+06 cycles, when eigenfrequency is reduced by 2%, (c) delamination became visible at N = 1,68E+06 cycles

Visual inspections of all samples subjected to vibration loading revealed delamination of the skin surface from the noodles at the root of the rib (Figure 11). This corresponds with the results obtained by vibrothermography and allows us to consider vibrothermography as a promising method of non-destructive testing for use in fatigue testing of composite structures.

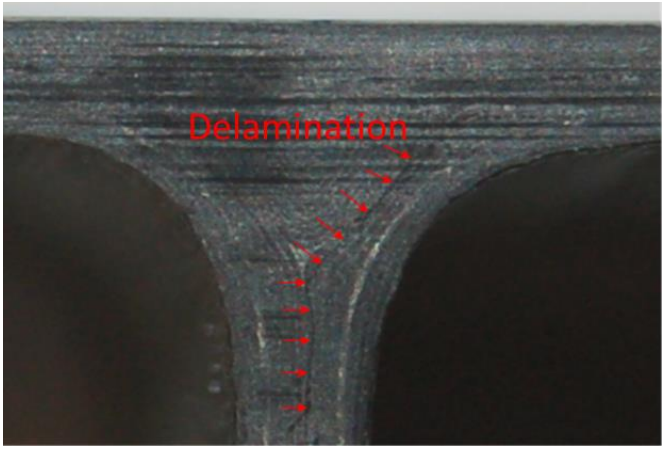

Figure 11 – Visually detectable delamination in the T-sample

7. Conclusions

The main result of the study of composite skin-stringer fatigue behavior is the data obtained by fatigue tests carried out on total 20 T-samples.

Based on the results of fatigue tests of T-samples under random narrow-band vibration loading, the S-N curve for a composite skin-stringer joint was plotted. A total of 10 virgin samples were tested at various levels of RMS strains. The S-N curve obtained is compared with the data from ESDU [3] for specimens of similar configuration (integral stringer).

Fatigue tests for a batch of 10 impacted T-samples were carried out under the same loading conditions, as for virgin samples. The comparison of the results for impacted and virgin samples has

shown that the impact damage of 5 J significantly reduces the durability of composite “skin-stringer” joint under random vibration loading.

The damage growth process in the T-sample was registered by non-destructive testing and data on the eigenfrequency reduction obtained from strain gauges. Using the results of vibrothermography and visual detection, the interllaminar crack in the joint between the skin and the stringer turned out to be the fundamental failure mode of the T-sample. The three different failure criteria were proposed, including 2% eigenfrequency reduction, 1-side visible delamination and 2-side visible delamination.

As part of development of a FEM for calculating the dynamic response of a T-sample, the modal and dynamic analysis for T-sample was carried out. The comparison of the FEM calculation results and experimentally measured data showed their good convergence. This makes it possible to use FEM analysis to study the dynamic response of similar structures under vibroacoustic loads.

8. Copyright Statement

The authors confirm that they, and/or their company or organization, hold copyright on all of the original material included in this paper. The authors also confirm that they have obtained permission, from the copyright holder of any third party material included in this paper, to publish it as part of their paper. The authors confirm that they give permission, or have obtained permission from the copyright holder of this paper, for the publication and distribution of this paper as part of the ICAS proceedings or as individual off-prints from the proceedings.

References

[1] B. L. Clarkson, Review of Sonic Fatigue Technology. NASA Contract Report, NASA–CR–4587 (National Aeronautics and Space Administration Langley Research Center, Hampton, VA, 1994).

[2] A. G. R. Thomson, Acoustic Fatigue Design Data. AGARDograph 162 (1972).

[3] ESDU 84027: Endurance of Fiber-Reinforced Composite, Laminated Structural Elements Subjected to Simulated Random Acoustic Loading (2014).

[4] Dubinskii, S., Feygenbaum, Y., Senik, V., & Metelkin, E. A study of accidental impact scenarios for composite wing damage tolerance evaluation. The Aeronautical Journal, 123(1268), 2019, p. 1724-1739

[5] S. V. Dubinskii, V. Ya. Senik, I. S. Sidorov & V. S. Dubinskii Determination of the Minimum Number of Inspections Necessary for Establishing of the Barely Visible Impact Damage Size in Composite Aeronautical Structures Journal of Machinery Manufacture and Reliability 49(1): 51-56, 2020

[6] Stanislav Dubinskii, Vitaliy Senik, and Yuri Feygenbaum "Field-Survey-Based Evaluation of Realistic and Remote Wing Impact Energy Levels", Journal of Aircraft, Vol.55, No. 6 (2018), pp. 2307-2312

[7] S. V. Dubinskii, F. S. Sevastyanov, A. Yu. Golubev, S. L. Denisov, V. M. Kostenko, I. A. Zharenov A Computational and Experimental Study of the Effect of Vibroacoustic Loads on the Structural Performance of Composite Skin-Stringer Joint. Acoustical Physics, 2019, Vol. 65, No. 4, pp. 359–368. DOI: 10.1134/S1063771019040043

[8] Y. Xiao, R. G. White, and G. S. Aglietti, Compos. Struct. 68, 455 (2005).

[9] Vavilov V.P., Chulkov A.O., Dubinskii S.V., Burleigh D., Shpilnoi V.Yu., Derusova D.A., Zhvyrblia V.Yu. Nondestructive testing of composite T-joints by TNDT and other methods. Polymer Testing, 94 (2021) 107012

[10] Dubinskii, S., Fedulov B., Feygenbaum, Y., Gvozdev, S., Metelkin, E. Experimental evaluation of surface damage relaxation effect in carbon-fiber reinforced epoxy panels impacted into stringer, Composites Part B (2019) 176 Article 107258

[11] K. J. Bathe and E. L. Wilson, J. Eng. Mech. Div., Am. Soc. Civ. Eng. 98, 1471 (1972).

[12] B. N. Parlett, The Symmetric Eigenvalue Problem (Prentice-Hall, Englewood Cliffs, NJ, 1980).

[13] LabWindowsTM/CVITM Programmer Reference Manual. National Instruments, Edition Part Number 323643A-01 (Austin, TX, 2003).

[14] A. I. Pankratov, A. V. Vrachev, A. A. Grigor'ev, V. I. Makarevich, N. A. Mozzherova, and V. S. Nikolaev, Manual for Airplane Designer, Vol. 3: Airplane Strength, Book 4: Fatigue Strength. Lifetime and Reliability of Airplane Frame, Issue 9: Procedure for Testing Aviation Structures under Acoustic Loading (Central Aero-Hydrodynamic Institute Named after Professor N. E. Zhukovsky 1981), No. 1292 [in Russian].

[15] Balageas, D., Maldague, X., Burleigh, D, Vavilov, V.P., Oswald-Tranta, B, Roche, J.-M., Pradere, C., Carlomagno, G.M. Thermal (IR) and Other NDT Techniques for Improved Material Inspection. Journal of Nondestructive Evaluation, Volume 35, Issue 1, 1 March 2016, pp. 1-17.